物 理 化 学 学 报

Acta Phys. -Chim. Sin. **2024,** *40* (X), 2308048 (1 of 14)

[Review] doi: 10.3866/PKU.WHXB202308048 www.whxb.pku.edu.cn

Research Progress on Cathode Electrolyte Interphase in High-Voltage Lithium Batteries

Jiandong Liu [1,2], Zhijia Zhang [3], Mikhail Kamenskii [4], Filipp Volkov [4], Svetlana Eliseeva [4], Jianmin Ma [1,*]

[1] School of Chemistry, Tiangong University, Tianjin 300387, China.

[2] School of Physics and Electronics, Hunan University, Changsha 410022, China.

[3] School of Material Science and Engineering, Tiangong University, Tianjin 300387, China.

[4] Institute of Chemistry, Saint Petersburg State University, Saint Petersburg 199034, Russia.

Abstract: Achieving high energy density batteries is currently a key focus in the field of energy storage. Lithium batteries, due to their high energy density, have garnered significant attention in research. Increasing the upper limit of the battery's cut-off voltage can boost the energy density of lithium batteries. However, high-voltage conditions can lead to irreversible phase transitions and side reactions in cathode materials, which can degrade battery performance and even result in safety risks, including explosions. The electrolyte can also decompose, causing capacity loss and releasing flammable gases when subjected to high voltage, which can lead to battery swelling and potential combustion and explosions. Designing an ideal cathode electrolyte interphase (CEI) on the cathode's surface to regulate the electrode-electrolyte interface reaction can effectively enhance the cycling stability of the battery, reduce irreversible phase transitions in the cathode, and improve the oxidation stability of the electrolyte. The ideal CEI should possess high ion conductivity, high thermal stability, and should minimize interface side reactions to ensure optimal battery performance. Understanding the formation and development of CEI is crucial for enhancing battery performance under high voltage. Apart from creating artificial CEI, modifying electrolytes has gained significant attention. By altering the electrolyte recipe, an ideal CEI can be achieved. Electrolyte engineering is considered an effective strategy for attaining an ideal CEI and enhancing the stability of high nickel positive electrodes. This approach is simple, cost-effective, and holds great promise for achieving higher energy density in lithium batteries. To provide a better understanding of CEI in lithium ion batteries (LIBs), this article reviews the latest advancements in CEI, including the formation mechanism of CEI, the key factors influencing CEI, methods for modifying CEI, and techniques for characterizing CEI. Additionally, it summarizes the current status of artificial CEI development and *in situ* CEI generation through electrolyte design. The aim is to offer fundamental guidance for future research and the design of high-voltage battery CEI. Finally, the article outlines the opportunities and challenges in electrolyte engineering for modified CEI, pointing towards the future direction of constructing an ideal CEI.

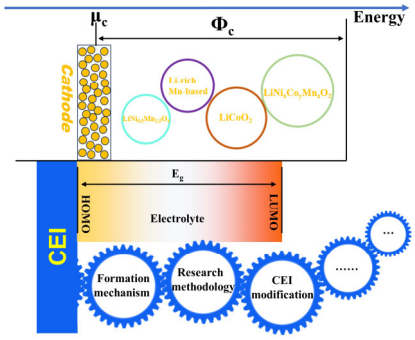

Key Words: High-voltage cathode; Cathode electrolyte interphase; Electrolyte engineering; Electrolyte additive; Lithium battery

Received: August 30, 2023; Revised: October 6, 2023; Accepted: October 30, 2023; Published online: December 20, 2023.

*Corresponding author. Email: nanoelechem@hnu.edu.cn

The project was supported by the National Natural Science Foundation of China (U21A20311).

国家自然科学基金(U21A20311)资助项目

高压锂电池正极电解质界面研究进展

刘建东[1,2]，张志佳[3]，Mikhail Kamenskii [4]，Filipp Volkov [4]，Svetlana Eliseeva [4]，马建民[1,*]

[1]天津工业大学化学学院，天津 300387

[2]湖南大学物理与微电子科学学院，长沙 410022

[3]天津工业大学材料科学与工程学院，天津 300387

[4]圣彼得堡国立大学化学研究所，圣彼得堡 199034，俄罗斯

摘要：提高电池的截止电压上限可以显著提升锂电池的能量密度。然而，高截止电压也会导致正极材料在高压下发生不可逆相变和副反应，从而损害电池性能。为了解决这一问题，建立一个稳定的正极电解质界面(CEI)在提高电池性能方面起到了关键作用。本文探讨了CEI的形成机制，并概述了构建CEI的方法，包括人工构建CEI和原位生成CEI。此外，从电解质的角度出发，我们还展望了构建高压正极CEI的设计思路。

关键词：高压正极；正极电解质界面；电解质工程；电解质添加剂；锂电池

中图分类号：O646

1 Introduction

In recent years, energy density of lithium-ion batteries (LIBs) has been pursued in response to the growing demand for portable electronic devices and electric vehicles [1]. While high-capacity electrode materials like silicon anodes and Li metal anodes play a crucial role, raising the upper voltage limit of current batteries is also a valuable approach to achieve high-energy-density LIBs [2–4]. Nevertheless, operating LIBs at high voltages can accelerate aging and reduce their cycle life. This is manifested in the decomposition of the electrolyte and the instability of cathode materials at high voltage [5–7]. Traditional carbonate electrolytes are usually decomposed *via* the oxidization when above 4.5 V is applied due to their low oxidation potential [8], which reduces the energy density of LIBs. In addition, cathode materials undergo irreversible changes such as phase transition, intergranular/intragranular microcracks, and transition metal cation dissolution and migration at high voltage, which will not only accelerate the battery failure, but also increase the safety hazards [9–11].

Various strategies, such as element doping [12–15] and surface coating [16–18], have been proposed to overcome the forementioned issues. Elemental doping can significantly enhance electronic/ionic conductivity, structural evolution, cation redox, and other properties closely related to electrochemical performance. Different doping strategies (e.g., doping elements, doping content, and doping sites) have been extensively explored to effectively improve the cathode performance at high voltage [14,19–21]. Surface coating is an effective way to protect the electrode surface, which can not only optimize the electrode surface structure for facilitating the charge transfer on cathode surface, but also act as the physical barrier between the electrode and electrolyte for enhancing the electrochemical kinetics [22–24]. It is effective to enhance battery cycling stability at high voltage through modulating the electrode-electrolyte interfacial reactions *via* designing cathode electrolyte interphase (CEI) on cathode surfaces. An ideal CEI should have high ionic conductivity, high thermal stability, and can avoid interfacial side reactions for ensuring battery performance [25,26]. The understanding of the formation and development of CEI is of great significance for improving battery performance at high voltage.

To gain a comprehensive understanding of CEI in LIBs, it is essential to review recent developments in this field. This includes the formation mechanism of CEI, the primary factors influencing CEI, the methods for modifying CEI, and the techniques for characterizing CEI (as shown in Fig. 1). Additionally, the current status of artificial CEI development and *in situ* CEI generation through electrolyte design is summarized. Our goal is to provide fundamental guidance for further research on the design of excellent CEI for high-voltage batteries.

2 Basic understanding of CEI

The significance of CEI has garnered increasing attention, primarily because an excellent CEI has the capacity to impede

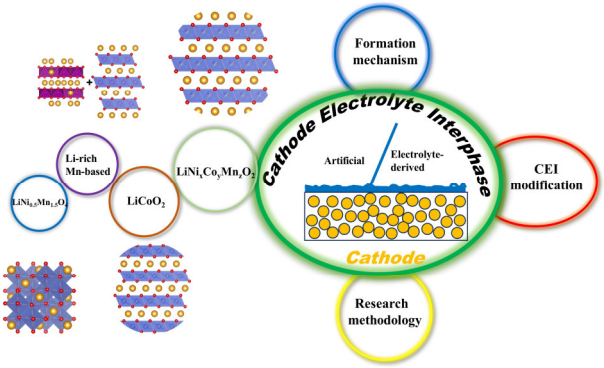

Fig. 1 The schematic research progress of CEI on high-voltage cathodes.

side reactions, especially during the continuous decomposition of electrolytes when LIBs work at high cut-off voltage. The CEI film comprises a combination of organic components like polycarbonate, alkyl lithium carbonate, alkyl lithium oxide, and inorganic components such as lithium carbonate, lithium fluoride, and lithium oxide [27]. The composition of the CEI film is intricate and intimately linked to the composition of the electrolyte. Therefore, a comprehensive understanding of the mechanisms behind CEI formation and the research methods involved is absolutely essential.

2.1 Formation mechanism of CEI

The history of research on CEI can be traced back to the observation of a $LiCoO_2$ surface layer by Goodenough using electron microscopy (as shown in Fig. 2a) [28]. Subsequently, Takehara *et al.* [29] found the existence of carboxylate groups on CEI surface using Fourier transform infrared spectroscopy (FT-IR, Fig. 2b). With the deeper understanding of CEI, the formation mechanisms of CEI begin to be understood. One view is that CEI is the decomposed products of the electrolytes on cathode surface. The highest occupied molecular orbital (HOMO) energy of solvent molecules is a qualitative evaluation index to measure the oxidation stability. It is generally believed that the higher the HOMO energy, the easier the molecule is to be oxidized. As shown in Fig. 2c, the movement of electrons and ions leads to a potential gradient at the interface between the electrode and the electrolyte during battery charging/discharging process. The Fermi level of electrode materials dictates their ability to gain and lose electrons. The Fermi level represents the highest energy level where an electron can occupy. On the cathode, the Fermi energy level of the cathode is lower than the HOMO energy of electrolyte components, then electrons are transferred from electrolyte components to the cathode, so that the electrolyte is oxidized and participates in the formation of CEI [30]. Both the solvents and salt in the electrolyte and corresponding decomposition products determine the composition and properties of CEI. Exploring the decomposition products is extremely important for understanding the properties of CEI. Fig. 2d shows a schematic diagram of possible oxidation reaction pathways after the initial oxidation of species in common electrochemical systems, where R represents hydrocarbons and X represents substituents [31]. For example, ethylene carbonate (EC) is a common cyclic solvent molecule, which undergoes a ring-opening reaction after losing electrons, and the decomposition products are mainly organic polymers and gases (e.g., $ROCO_2Li$ and CO_2). The decomposition products of $LiPF_6$ are mainly LiF and $Li_xPO_yF_z$. In addition, it should be noted that the HF by-product generated by the decomposition of $LiPF_6$ will cause the dissolution of cathode transition metal ions. Moreover, dissolution the material leads to cyclic instability of the coin-cells.

An alternative perspective suggests that the formation of CEI is attributed to electrolyte decomposition and compositional migration from solid electrolyte interphase (SEI) [32]. Li *et al.* [33] analyzed the relationship between the CEI on $LiCoO_2$ surface and the SEI composition on the anode surface by X-ray photoelectron spectroscopy (XPS). Fig. 3a shows the change

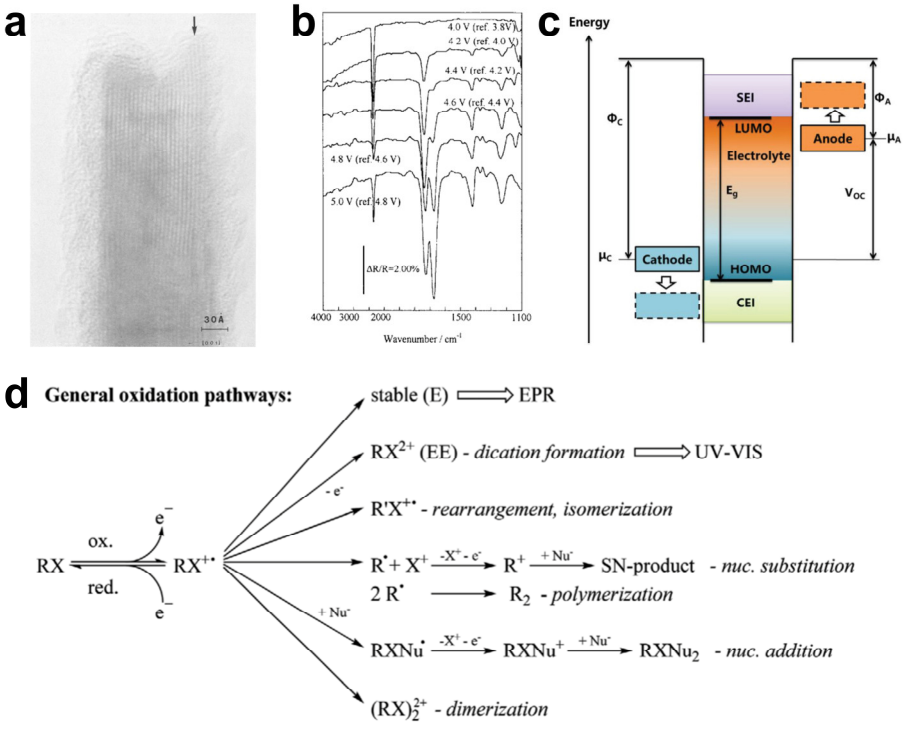

Fig. 2 (a) Surface layer observed on $LiCoO_2$ surface by electron microscope [28]; (b) infrared Spectrum of Surface Layer Observed on $LiCoO_2$ Surface [29]; (c) energy schematic diagram of between electrode and electrolyte [30]; (d) schematic diagram of the possible oxidation reaction pathways after the initial oxidation of species in common electrochemical systems [31].

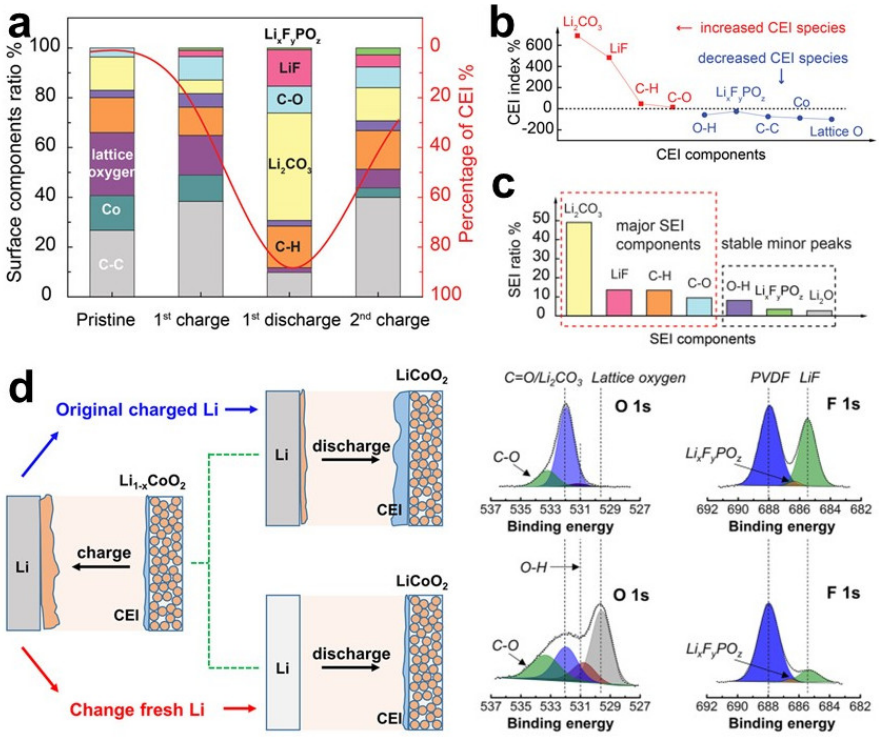

Fig. 3 (a) The chemical composition of the $LiCoO_2$ interface layer is detected by XPS under different charging and discharging states of the cathode, the red curve basically indicates the evolution of CEI species in the battery cycle; (b) the main components of CEI obtained through quantitative XPS analysis; (c) the chemical composition of lithium anode SEI layer; (d) study the schematic diagram of the interaction between cathode and anode and the corresponding XPS diagram of $LiCoO_2$ surface CEI [33].

trend of the composition of CEI during battery cycling process. As shown Fig. 3b,c, the change trend of the main components of CEI increase basically reproduces the content distribution of the corresponding SEI components on anode surface, which indicates the correlated relationship between the cathode and the anode. However, only a slight change in the CEI composition after replacing a new anode in the charged state further supports this conclusion (Fig. 3d).

While the formation mechanism of CEI remains a subject of debate, it is undeniable that an excellent CEI is the result of a synergistic effect among various components to ensure optimal battery performance. The formation of CEI is associated with several factors, including the battery's cut-off voltage, changes in the cathode structure, and the charge-discharge rate. Notably, when the upper cut-off voltage of the battery is increased, it simultaneously increases the battery's capacity and the dissolution of more excessive transitional metal ions. This, in turn, can lead to phase changes in the cathode and the continuous decomposition of the electrolyte, resulting in the formation of a non-uniform thickness CEI. Therefore, designing an excellent CEI at high voltage is of great significance for stable battery cycling.

2.2 Research methodology of CEI

The rapid development of characterization techniques offers effective means to gain a deeper understanding of CEI deeply. The commonly used characterization methods can be divided into morphological characterization, component characterization, and theoretical analysis. The main methods for morphological characterization include scanning electron microscopy (SEM), transmission electron microscopy (TEM), cryo-electron microscopy (cryo-EM), electrochemical atomic force microscopy (EC-AFM), *etc*. The main methods for component characterization include XPS, time-of-flight secondary ion mass spectrometry (TOF-SIMS), *etc*. XPS is a surface analysis method that provides the content and morphology of elements on the surface of a sample, rather than the composition of the whole sample. SEM and TEM are common characterization methods for studying the morphology of CEI (Fig. 4a) [34]. The sample characterized by SEM is relatively simple to prepare, can be dynamically observed and has high resolution, but it has the following disadvantages: the resolution is lower than TEM, and the sample needs to be observed in a vacuum environment, which limits the type of sample; only the surface morphology of the sample can be observed, and the structures below the surface cannot be detected. There is no height direction information, only two-dimensional plane image; Liquid samples cannot be observed. TEM has high resolution and can be used to observe the crystal lattice on the crystal surface, but it has certain destructive effects on the sample and high material requirements. In addition, the observation range of TEM is small, and the sample area tested in the experiment only accounts for a small part of the overall material, which could not totally reflect the material situation. XPS is used to analyze the chemical evolution of the CEI layer by testing the binding energy of elements to

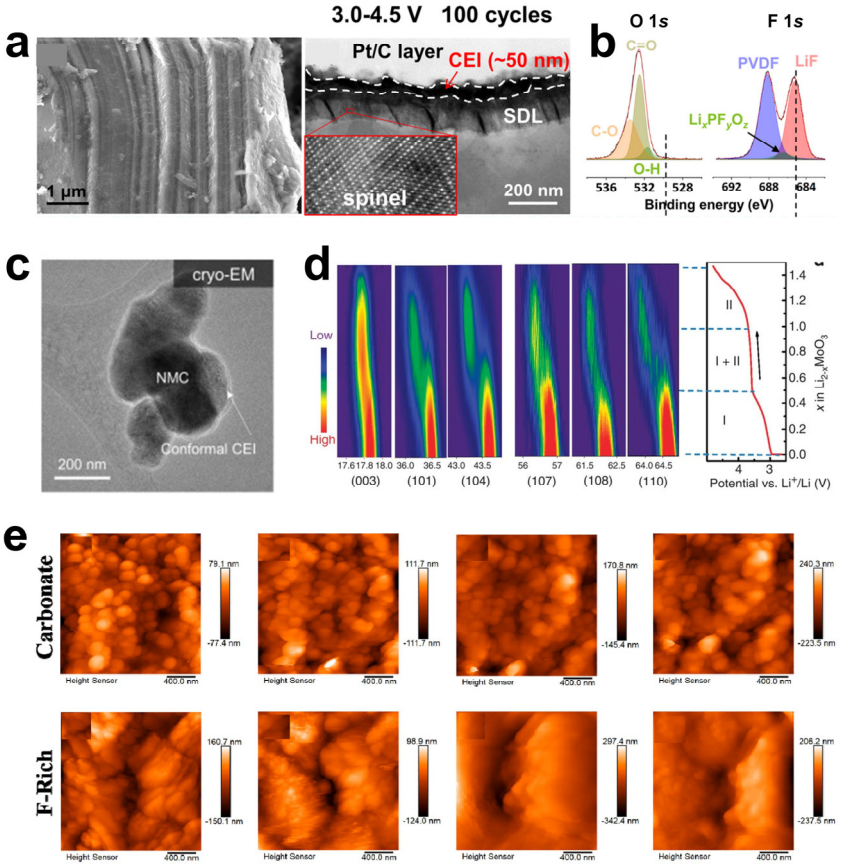

Fig. 4 (a, b) SEM and TEM images of $LiCoO_2$ cathode after 100 cycles at 3–4.5 V, as well as XPS spectra of CEI [34]; (c) the uniform CEI layer on the surface of NMC observed by cryo-EM [25]; (d) evolution diagram of diffraction peaks of $Li_{2-x}MoO_3$ during lithium removal at 4.8 V voltage [35]; (e) *in situ* AFM images of cathodes in carbonate electrolytes and F-generation carbonate electrolytes [36].

analyze the types and contents of elements on the sample surface (Fig. 4b).

XPS is more convenient to analyze the valence states of elements through the binding energy displacement of elements and has better quantitative ability and is more widely used. However, because it is not easy to focus and the irradiation area is large, the average value obtained is within the millimeter diameter range, and the detection limit is generally only 0.1%, so the measured object on the surface of the material is required to be several orders of magnitude larger than the actual amount analyzed. Cryo-EM is a microscopic technique that uses a transmission electron microscope to observe samples at low temperatures. The advantages and disadvantages of cryo-electron microscopy are as follows: the microstructure of the sample can be made close to the living state by freezing. After freezing fracture etching, the microstructure of different split surfaces can be observed, and the membrane structure and inclusions in cells can be studied. The freeze-etched sample, the replica film prepared by platinum and carbon spray plating has a strong three-dimensional sense and can withstand electron beam bombardment and long-term preservation. However, freezing can also cause artificial damage to samples. The fracture surface is mostly generated in the most vulnerable part of the sample structure, which cannot be selected purposefully. Cui *et al.* [25] used cryo-EM to study the CEI in standard carbonate electrolytes on the atomic scale (Fig. 4c).

X-ray diffraction analysis (XRD) is an effective method for studying the microstructure of crystalline and some amorphous substances. It is a common material characterization method for researchers, offering high analysis speed without altering the chemical state of the sample or causing sample flight. XRD can analyze solid, powder, and liquid samples with good reproducibility. Sample preparation is simple, solid, powder, liquid samples can be analyzed. Its disadvantage is that it is difficult to make absolute analysis, and quantitative analysis needs standard samples; it is less sensitive to light elements; It is easily affected by mutual element interference and superposition peaks. Fig. 4d demonstrates the use of *in situ* XRD to characterize the crystal structure of the material and its phase transition process [35]. AFM is a kind of scanning probe microscope. Compared with SEM, AFM has many advantages. Unlike electron microscopy, which can only provide two-dimensional images, AFM provides a true three-dimensional surface map. Cai *et al.* [36] showed by EC-AFM that fluorinated electrolytes form uniform CEI at high voltage (Fig. 4e). However, AFM does not require any special treatment of the sample, such as copper plating or carbon plating, which can cause irreversible damage to the sample. Third, electron

microscopes need to operate in high vacuum conditions, and atomic force microscopes work well at atmospheric pressure. Compared with SEM, the shortcomings of AFM are that the imaging range is too small, the speed is slow, and the influence of the probe is too great.

XAS can be applied for more accurate identification of atomic structures and can provide valuable information about the coordination environment and the chemical state of the detected atom. XAS materials do not need to possess a good crystal structure or a long-range ordered structure. XAS testing has very low sample requirements and will not damage the sample. The first cycle of (de)lithiation mechanism in NCM622 was extensively described by Takeuchi *et al.* [37] using X-ray absorption near-edge structure (XANES) analysis and extended X-ray absorption fine structure modeling (EXAFS). The electrochemical participation and structural changes of transition metals indicate that the redox behavior of Ni is the main reason for the structural deformation of cathode materials (Fig. 5a). However, XAS has limitations in that it can only provide a planar average structure and cannot offer three-dimensional information. TOF-SIMS has high resolution, high sensitivity, accurate mass measurement, and other properties, making it widely used in high-tech analysis. TOF-SIMS has high detection sensitivity, which can reach the detection sensitivity of up to ppm/ppb, and has high quality resolution, which can observe the sample component distribution in a more three-dimensional manner. Its disadvantage is that it will cause little damage to the sample sputtering; the sample to be tested is mainly solid at present; Powder samples can only be tested for spectrograms and cannot be analyzed in depth. TOF-SIMS can be used to explore the CEI structure more intuitively. As shown in Fig. 5b, the 3D fragments and distributions of C_2HO^- and BO_2^- indicate that the additives can reduce the decomposition of EC and EMC on the cathode surface and generate a more uniform CEI. The advantages and disadvantages of the above methods was summarized in the Table 1.

Quantum calculation (QC), density functional theory (DFT), classical molecular dynamics (CMD), *ab initio* molecular dynamics (AIMD) are commonly used, together with popular machine learning (Fig. 6). Solvents, lithium salt and additives in the electrolyte can be studied by QC to explore bulk and microscopic characteristics, such as surface electrostatic potential of additives (Fig. 6a) [39]. Additionally, redox potential, bond dissociation energy, reaction energy, transition state, and reaction energy barrier of these components can be calculated through QC to assist in understanding and predicting the behavior of the electrolyte. Commonly used QC software include Gaussian, ORCA, *etc.* [40,41]. The electronic structure (density of states and energy bands), adsorption, charge density difference, Bader charge, work function, diffusion path, diffusion energy barrier, ion conductivity, charge discharge curve, probability density distribution of electrode materials can be calculated through DFT. Commonly used DFT software includes VASP, Quantum ESPRESSO, CP2K, and Cystal, *etc.* [42,43]. For example, DFT can study the adsorption behavior of electrolyte components on the surface of electrode materials,

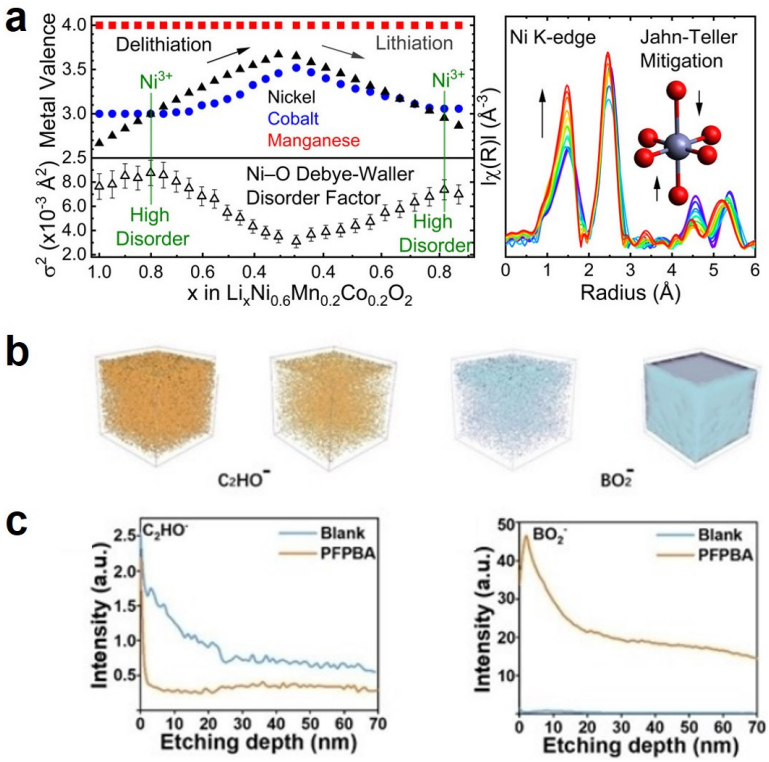

Fig. 5 (a) The average Ni, Co, and Mn valences in the first cycle of fresh cells, as well as the EXAFS spectra during the first discharge of Ni *K*-edge [37]; (b, c) 3D fragments and distribution of C_2HO^- and BO_2^- on NCM622 Surface CEI in different electrolytes observed by TOF-SIMS [38].

Table 1 A summary table of the advantages and disadvantages of the above methods.

Methods	Advantage	Disadvantage
XPS	Provides the content of elements on the surface/ analyze the valence states of elements/ better quantitative ability	Not easy to focus/ the large irradiation area/ the detection limit
SEM	Simple to prepare samples/ dynamically observed/ high resolution	The lower resolution/ vacuum environment limits the type of sample/ only the surface morphology observed/ no height direction information/ not liquid samples
TEM	High resolution/ observing the crystal lattice on the crystal surface	Certain destructive effects on the sample/ high material requirements/ small observation range
Cryo-EM	Close to the living state/ observing microstructure of different split surfaces/ withstanding electron beam bombardment and long-term preservation	Artificial damage to samples/ Limitations of observation area selection
XRD	High analysis speed/ no extra changes in the chemical state/ measured repeatedly with good reproducibility/ simple sample preparation	Poor absolute analysis/ quantitative analysis needs standard samples/ less sensitive to light elements/ easily affected by mutual element interference and superposition peaks
AFM	True three-dimensional surface map/ not require any special treatment of the sample/ work well at atmospheric pressure	Small imaging range/ slow speed/ great influence of the probe
XAS	More accurate atomic structure identification/ the coordination environment and the chemical state/ low sample requirements/ nondestructive	Only the planar average structure and no three-dimensional information
ToF-SIMS	High resolution/ high sensitivity/ accurate mass measurement/ three-dimensional manner	Little damage to the sample/ mainly solid at present

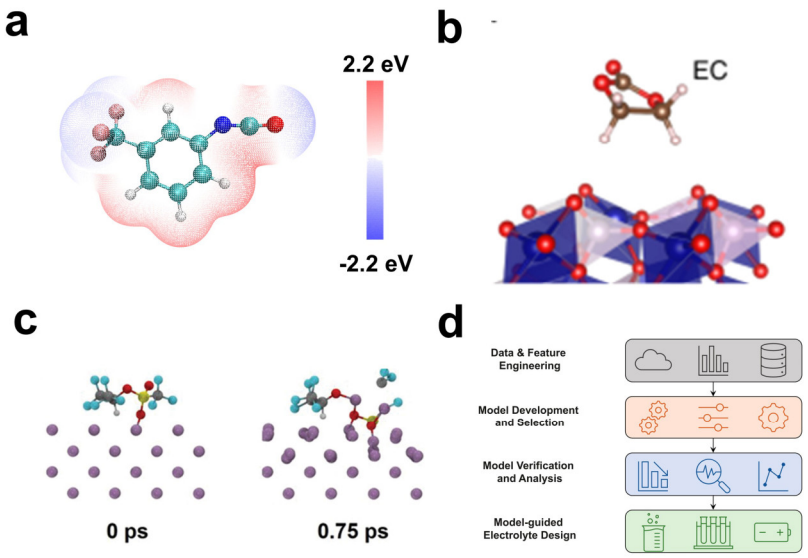

Fig. 6 Commonly used calculation methods in the study of CEI. (a) QC calculation of surface electrostatic potential of additives [39]; (b) DFT calculation of adsorption on the cathode [44]; (c) CEI formation simulation with AIMD [45]; (d) Machine learning in the electrolyte field of batteries [46].

and then change the decomposition behavior of electrolyte components for affecting the composition of CEI (Fig. 6b) [44]. In addition, the Li^+ migration behavior in CEI can be studied by DFT calculations. Molecular dynamics simulations enable the study of the Li^+ solvation structure in the electrolyte and the interfacial behavior between the electrode and the electrolyte. The formation of CEI is affected by the Li^+ solvation structure. AIMD has a powerful function to study the Li^+ migration energy barrier in CEI and the Li^+ solvation structure of in the electrolyte, and can also directly simulate the generation process of CEI (Fig. 6c) [45]. However, the cost is high, which is limited by the size of AIMD simulation system and the duration of the simulation. Compared to AIMD, CMD can simulate larger systems and longer simulation times. Commonly used CMD software include GROMACS, LAMMPS and DL_POLY, *etc*. Classical MD can simulate the solvation structure, ion conductivity, viscosity, *etc*. of electrolyte systems, helping to understand the microscopic behavior of electrolytes. However, CMD relies on the selection of force fields, and a good force field can accurately simulate the behavior of the electrolyte, such as OPLS-AA force field. Thanks to the rapid development of machine learning and databases in recent years, data-driven battery research has gained widespread attention (Fig. 6d) [46]. Database-based high-throughput screening combined with machine learning, can not only quickly screen out suitable solvents or additives from thousands of organic solvents, but also discovers new CEI models and CEI formation mechanisms for accelerating developing battery electrolyte.

Currently, various characterization methods have been applied to characterize CEI, and the interfacial reaction mechanism can be effectively combined with theoretical calculations, assisting in constructing a stable CEI to ensure high-performance LIBs.

3 Development of CEI

According to the structure, commonly used high-voltage cathode materials for LIBs include $LiCoO_2$ and $LiNi_xCo_yMn_zO_2$ with a layered structure (NCM), $LiNi_{0.5}Mn_{1.5}O_4$ (LNMO) with a spinel structure, and Li-rich Mn-based cathode (LMR). The cathode materials in LIBs face many challenges when they work at high voltage, such as the phase transition of the material structure, the formation of crystal cracks, and the migration of transition metal ions [2]. These unexpected changes will lead to the limitation of the capacity of the cathode material and the decomposition of the electrolyte, increase the battery impedance and even lead to battery failure. Forming excellent CEI on the surface of cathode materials is an effective way to solve this problem. In recent years, people have gradually realized the importance of CEI and conducted a lot of research, which mainly focused on the construction of artificial CEI and adjusting the electrolyte to facilitate the *in situ* generation of CEI. Artificial SEI refers to the generation of an external interphase on the electrode surface through thin film techniques such as chemical vapor deposition, atomic layer deposition, and sputtering. *In situ* SEI refers to the *in situ* interface layer derived from the redox reaction of the electrolyte in the battery. This part will summarize the formation method and effect of CEI.

3.1 Formation of artificial CEI

Artificially coated CEI demonstrates a protective effect on cathode materials at high voltage, such as metal oxides [47,48], fluorides [49], phosphates [50], and others. These coating materials can effectively reduce the reaction between the cathode and electrolyte for inhibiting the dissolution of transition metal ions. For example, Lee *et al.* [51] deposited MgF_2 on $LiCoO_2$ surface by co-precipitation technique, which not only increased the stability of the cathode during cycling at 4.5 V, reduced the dissolution of Co^{2+}, but also increased the thermal stability of the electrode. The amorphous zirconia modified NCM622 cathode prepared by Yang *et al.* [52] effectively stabilized the CEI and suppressed the structural degradation, and the unique porous framework also provided a large amount of activity site on the NCM622 surface, which made 4.5 V Li||NCM622 battery to realize a capacity retention of 82.5% after 100 cycles. Although these common artificial CEI can protect the cathode at high voltage to a certain extent, the thickness, uniformity and compactness of the coating cannot be guaranteed and the differences in the working mechanism of different coatings limit the electrode optimization. Therefore, it is of great significance to develop new coating materials and explore the mechanism of action of coating materials.

In addition to the above three common artificial CEI, various new artificial CEIs have been studied in recent years. Wang *et al.* [27] successfully constructed a layer of artificial Li^+ conductor cathode-electrolyte interphase (ALCEI) on NCM811 surface by using the nucleophilic reaction between polysulfide ions (Li_xS_8) and vinylene carbonate (VC), as shown in Fig. 7. The ALCEI modified layer has good mechanical strength and flexibility and high ionic conductivity, which effectively prevents the penetration of the electrolyte and inhibits the side reactions at the interface, thereby eliminating the irreversible phase transition on the surface for improving the electrochemical reversibility at 4.5 V. Besides, utilizing conductive polymers as artificial CEIs can not only improve the conductivity of the electrode by utilizing

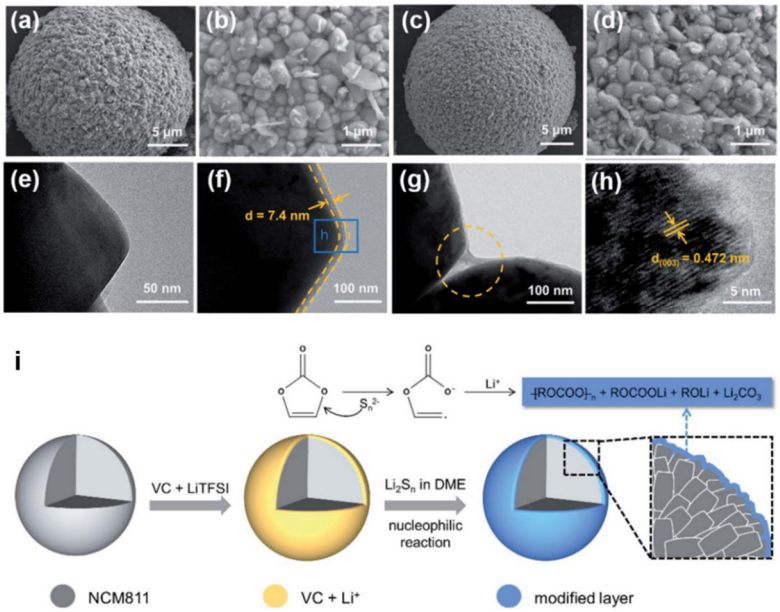

Fig. 7 SEM images of (a, b) pristine and (c, d) ALCEI-modified cathode; TEM images of (e, f) pristine and (g, h) ALCEI-modified NCM811; (i) schematic diagram of the formation of ALCEI-modified NCM811 [27].

its conductive network, but also stabilize the cathode surface. Zhao *et al.* [53] achieved stable cycling and high Coulombic efficiency by depositing a polypyrrole on LNMO surface. The conductive layer can not only enhance the electronic conductivity, suppress the dissolution of Mn^{4+} and Ni^{2+} during cycling process, but also avoid the electrolyte decomposition on cathode surface. Although artificial CEI can effectively protect the cathode stability during cycling at 4.9 V, compared with the *in situ* generation of CEI by adjusting the electrolyte. In the future, it is expected to study more simple and effective methods for constructing artificial CEI.

3.2 Electrolyte engineering derived CEI

By introducing different anions into the Li^+ solvation structure, such as high concentration electrolytes (HCEs), local high concentration electrolytes (LHCEs), and weak solvation electrolytes (WSEs), the CEI formation process can be reasonably controlled. HCE electrolytes and ionic liquids are also used in high-voltage LIBs, but both electrolytes have high viscosity, which greatly reduces the wettability of the electrolyte into the electrodes [54]. Additionally, fluorinated electrolytes are used to explore the high-voltage performance of LIBs. However, due to their high cost, using conventional carbonate electrolytes with additives is a more economical choice. This section primarily focuses on CEI-forming additives for conventional carbonate electrolytes, which can be categorized into inorganic and organic additives based on their structures.

Common organic additives include F-containing additives, B-containing additives, P-containing additives, Si-containing additives, and N-containing unsaturated molecule additives [55–59]. These specific elements are often referred to as “favorable elements.” Compared to solvent molecules, these additive molecules have a higher HOMO value, so they are easily oxidized prior to solvent molecules for participating in the formation of CEI. F-containing additives are the most common film-forming additives. F atoms can significantly reduce the electron density of adjacent atoms, because low electron density is associated with good oxidation stability, so fluorination is considered to be a way to enhance the cathode stability of commercial electrolyte solvents. F-containing additives are extremely easy to be oxidized on the cathode surface to generate CEI containing LiF [60,61]. LiF-rich CEI possesses a high density, which is beneficial for protecting the cathode and reducing the deformation and formation of cracks on the cathode surface [62]. Fig. 8a summarizes common fluorinated additives and their applications [63].Common B-containing additives mainly include trimethyl borate, triethyl borate, *etc.*, because the boron atom lacks electrons, it is easy to coordinate with the anion PF_6^-, thereby reducing the oxidation potential of the basic electrolyte and participating in the formation of protective CEI (Fig. 8b) [64,65]. Besides, the use of cobalt free LMR cathode materials can achieve excellent electrochemical performance at high voltage with the help of electrolyte additives, such as ionic liquids containing abundant “favorable elements” [66].

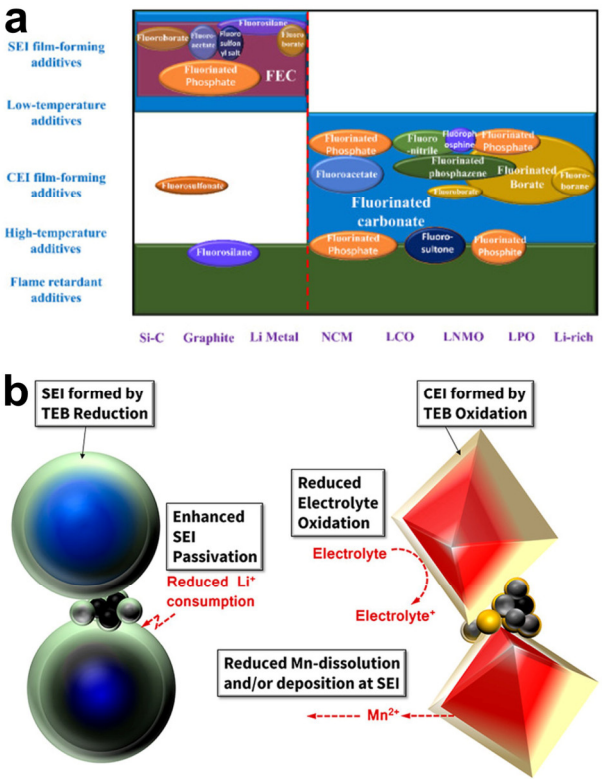

Fig. 8 (a) Common fluorine-containing additives and their applications [63]; (b) schematic diagram of the role of triethyl borate additives [64].

P-containing additives can not only form an excellent CEI film, but also have flame-retardant effect. For example, common P-containing additives include tris(pentafluorophenyl)phosphine (TPFPP), trimethyl phosphate, triethyl phosphate, *etc.* [67–69]. As shown in Fig. 9a, tris(trimethylsilyl)phosphate as an additive can form ionically conductive and robust P- and Si-rich SEI/CEI on both anode and cathode [70]. Nitrile additives are commonly viewed as N-containing unsaturated additives. 3-(trifluoromethyl)benzoylacetonitrile with the multifunctional combination of phenyl, nitrile and fluoride groups enabled Li||NCM811 batteries to exhibit stable electrochemical performance at 5 V [71]. Triallyl isocyanurate was introduced as a novel electrolyte additive to enhance the performance of $LiCoO_2$ cathodes at 4.5 V [72].

Some Li salts are also used as high-voltage additives. Inorganic Li salts mainly include lithium perchlorate ($LiClO_4$), tetrafluoroborate ($LiBF_4$), hexafluoroarsenate ($LiAsF_6$), and hexafluorophosphate ($LiPF_6$). $LiClO_4$ has been studied with the longest research history because of appropriate conductivity, thermal stability, and oxidation resistance stability. However, due to its strong oxidant nature, it is only suitable for practical batteries from safe viewpoint. $LiBF_4$ is used as Li salt additive with a wide operating temperature range, good stability at high temperatures, and excellent low-temperature performance. $LiBF_4$ can also enhance the film-forming ability on the electrode for inhibiting Al foil corrosion. However, the ion conductivity of $LiBF_4$ based electrolyte is lower due to the small radius of BF_4^-

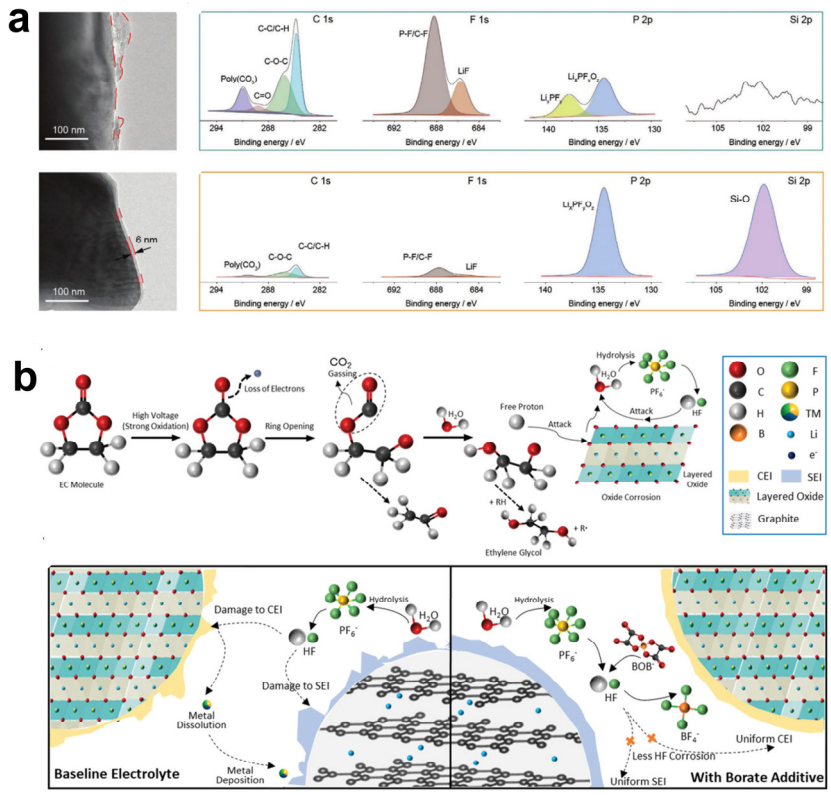

Fig. 9 (a) TEM images and XPS spectra of CEI on NCM811 cathode after cycling in blank electrolyte (EC/DEC) and electrolyte containing tris (trimethylsilyl) phosphate ester additives [70]; (b) mechanism diagram of LiBOB as an additive [73].

and its difficulty in dissociation, which limits the application of $LiBF_4$ as main Li salt in electrolytes. Among known Li salts, $LiAsF_6$ can demonstrate the best cycling performance, relatively good thermal stability, and almost the highest conductivity. However, the potential carcinogenic effect of arsenic element limits their application. $LiPF_6$ has good electrochemical stability, does not corrode the current collector, and is easily soluble in organic solvents such as carbonates. Meanwhile, due to the large radius of PF_6^- and weak synergistic effect at room temperature, $LiPF_6$ solution has high ionic conductivity. Despite its poor thermal stability and easy hydrolysis, $LiPF_6$ is still the most widely used and commercially valuable among the four traditional inorganic Li salts. In addition, some new organic Li salts have been proposed as additives for LMBs. For example, Li bis(oxalate)borate (LiBOB) as an additive can ensure the excellent cycling stability of the battery, because the LiBOB salt or borate radicals generated by the decomposition of LiBOB can effectively act as HF scavengers by forming B—F species, which in turn a more uniform and stable CEI is generated to ensure stable battery cycling at high voltage (Fig. 9b) [73]. Li difluorophosphate as an electrolyte additive can build an organic-inorganic hybrid interphase on both the cathode and anode for improving the battery performance [74]. In addition, other inorganic additives also have a protective effect on the cathode. As shown in Fig. 10a, Zheng *et al.* [75] utilized a trace amount of potassium selenocyanate (KSeCN) (0.1%, wt) as an additive to endow Li||$LiCoO_2$ batteries with excellent cycling performance at a charge cut-off voltage of 4.6 V, since this additive built stable and dense SEI/CEI films through the synergistic effect with —Se and —C≡N groups for uniform Li deposition and stabilizing $LiCoO_2$ during cycling process. Xu *et. al.* [76] used LiBOB for enhancing the performance of LNMO cathode at 4.8V and inhibiting the dissolution of Mn/Ni upon cycling. Besides, novel Li borate additives were designed for the surface modification of high-voltage LNMO cathodes (Fig. 10b,c), such as Li 2-fluorophenol trimethyl borate (LFPTB), Li 4-pyridyl trimethyl borate (LPTB) and Li trimethylsilyl trimethyl borate (LTSTB) [77].

The synergistic effect of different functional groups of electrolyte additives or of multiple additives can lead to better performance than an induvial additive [79]. The synergistic effect of co-additives of suberonitrile or 1,3,6-hexanetrinitrile and FEC resulted in a thin and uniform CEI on $LiCoO_2$ surface at 4.6 V [78]. The lone electron pair on the N 2*p* orbital of nitrile reduces the catalytic effect of Co^{3+}/Co^{4+} in the electrolyte while FEC is beneficial to the formation of an electronically insulating interfacial layer containing LiF, which lead to Li||$LiCoO_2$ batteries with stable cycle performance (Fig. 10d).

In addition, there are many electrolyte designs that can significantly improve the performance of practical pouch cells, with high battery energy density and long cycle life [80]. However, due to the level of laboratory equipment, most research is still limited to button batteries. However, to achieve commercialization, testing of pouch cells is essential. So future

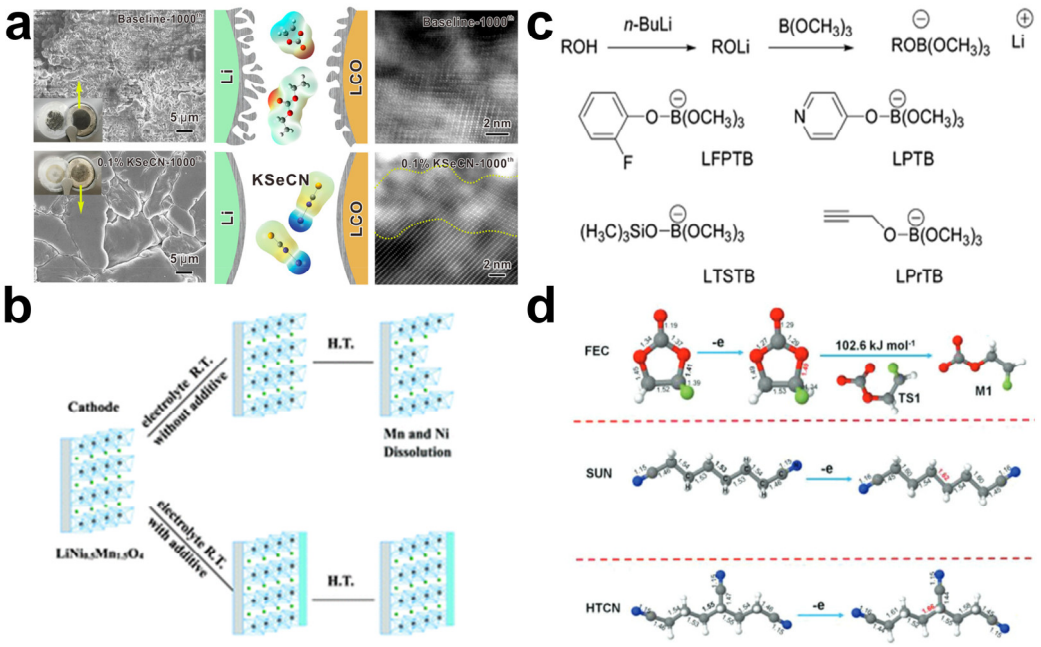

Fig. 10 (a) The mechanism diagram of the action of potassium selenocyanate as an additive [75]; (b) the structural evolution of LNMO with or without electrolyte additives [77]; (c) development route of new boron containing electrolyte additives [77]; (d) the formation mechanism of CEI membrane in electrolytes containing synergistic additives (benzonitrile or 1,3,6-hexatrienitrile with FEC) [78].

research needs to conduct comprehensive testing and characterization of pouch cells to further move towards the commercialization.

In summary, designing an excellent CEI through electrolyte additives is of great significance for stable battery cycling at high voltage. Based on above work, the requirements on designing high-voltage additives can be summarized: i) have a higher HOMO value than the electrolyte solvent for being preferentially oxidized than the electrolyte solvents; ii) have high solubility and stability in the electrolyte; iii) have stable decomposition products; iv) have some important functional groups (e.g., B-, F-, Si-, P- and N-based unsaturated molecules) for functional CEI; vi) can remove trace impurities (e.g., HF or water) in the electrolyte.

4 Summary

Excellent CEI is crucial for stable cycling of high-voltage LIBs. The ideal CEI should have the following properties: i) has high Li^+ conductivity; ii) is uniform and stable, can suppress the dissolution of excessive metals and can suppress the generation of gas; iii) inhibits the phase transition of the cathode material; vi) prevents the occurrence of interface side reactions. There have been a variety of instrumental characterizations and theoretical simulations to explore the composition mechanism of CEI. In addition, many researchers are committed to constructing CEI with excellent cathode surface stability under high voltage, including the design of artificial CEI, the design of anti-oxidation solvent, and the development of CEI-forming additives. The design of artificial CEI mainly aims to develop and utilize various advanced thin film technologies, such as physical vapor deposition. The design of antioxidant solvents is crucial as they can broaden the electrochemical window of the electrolyte and generate high voltage resistant CEI. Film forming additives are a relatively simple and economical way, and there is an urgent need to develop new additives. Future research on high-voltage CEI needs to focus on the following issues: i) the composition and thickness of CEI need to be precisely constructed; ii) the formation mechanism of CEI needs to be explored in combination with more *in situ* characterization techniques; iii) developing more effective strategies for constructing CEI; iv) using machine learning to screen cathode materials and electrolytes that are stable at high voltage can accelerate the practical application of high-voltage LIBs. We believe that with the development of science and technology, the CEI on the cathode surface under high voltage will be fully explored and improved, and the practical application of high-energy-density batteries is just around the corner.

Author Contributions: Conceptualization, J.D. Liu and J.M. Ma; Methodology, J.D. Liu; Software, J.D. Liu; Validation, J.D. Liu; Formal Analysis, J.D. Liu and Z.Z. Zhang; Investigation, J.D. Liu; Writing - Original Draft Preparation, J.D. Liu; Writing – Review & Editing, M. Kamenskii, F. Volkov, S. Eliseeva; Visualization, J.D. Liu; Supervision, J.M. Ma; Project Administration, J.M. Ma; Funding Acquisition, J.M. Ma.

References

(1) Goodenough, J. B.; Park, K.-S. *J. Am. Chem. Soc.* **2013,** *135*, 1167. doi: 10.1021/ja3091438

(2) Jia, H.; Xu, W. *Trends Chem.* **2022,** *4*, 627. doi: 10.1016/j.trechm.2022.04.010

(3) Wu, Y.; Liu, X.; Wang, L.; Feng, X.; Ren, D.; Li, Y.; Rui, X.; Wang, Y.; Han, X.; Xu, G.-L.; *et al. Energy Storage Mater.* **2021,** *37*, 77. doi: 10.1016/j.ensm.2021.02.001

(4) Pham, H. Q.; Chung, G. J.; Han, J.; Hwang, E.-H.; Kwon, Y.-G.; Song, S.-W. *J. Chem. Phys.* **2020,** *152*, 094709. doi: 10.1063/1.5144280

(5) Zhang, J.; Wang, P.-F.; Bai, P.; Wan, H.; Liu, S.; Hou, S.; Pu, X.; Xia, J.; Zhang, W.; Wang, Z.; *et al. Adv. Mater.* **2022,** *34*, 2108353. doi: 10.1002/adma.202108353

(6) Li, W.; Song, B.; Manthiram, A. *Chem. Soc. Rev.* **2017,** *46*, 3006. doi: 10.1039/C6CS00875E

(7) Kong, D.; Hu, J.; Chen, Z.; Song, K.; Li, C.; Weng, M.; Li, M.; Wang, R.; Liu, T.; Liu, J.; *et al. Adv. Energy Mater.* **2019,** *9*, 1901756. doi: 10.1002/aenm.201901756

(8) Ren, X.; Chen, S.; Lee, H.; Mei, D.; Engelhard, M. H.; Burton, S. D.; Zhao, W.; Zheng, J.; Li, Q.; Ding, M. S.; *et al. Chem* **2018,** *4*, 1877. doi: 10.1016/j.chempr.2018.05.002

(9) Song, S. H.; Cho, M.; Park, I.; Yoo, J.-G.; Ko, K.-T.; Hong, J.; Kim, J.; Jung, S.-K.; Avdeev, M.; Ji, S.; *et al. Adv. Energy Mater.* **2020,** *10*, 2000521. doi: 10.1002/aenm.202000521

(10) Piao, Z.; Gao, R.; Liu, Y.; Zhou, G.; Cheng, H.-M. *Adv. Mater.* **2023,** *35*, 2206009. doi: 10.1002/adma.202206009

(11) Qin, Y.; Cheng, H.; Zhou, J.; Liu, M.; Ding, X.; Li, Y.; Huang, Y.; Chen, Z.; Shen, C.; Wang, D.; *et al. Energy Storage Mater.* **2023,** *57*, 411. doi: 10.1016/j.ensm.2023.02.022

(12) Sun, H. H.; Kim, U.-H.; Park, J.-H.; Park, S.-W.; Seo, D.-H.; Heller, A.; Mullins, C. B.; Yoon, C. S.; Sun, Y.-K. *Nat. Commun.* **2021,** *12*, 6552. doi: 10.1038/s41467-021-26815-6

(13) Zhou, K.; Xie, Q.; Li, B.; Manthiram, A. *Energy Storage Mater.* **2021,** *34*, 229. doi: 10.1016/j.ensm.2020.09.015

(14) Li, J.; Li, W.; Wang, S.; Jarvis, K.; Yang, J.; Manthiram, A. *Chem. Mater.* **2018,** *30*, 3101. doi: 10.1021/acs.chemmater.8b01077

(15) Xie, Q.; Li, W.; Dolocan, A.; Manthiram, A. *Chem. Mater.* **2019,** *31*, 8886. doi: 10.1021/acs.chemmater.9b02916

(16) Nisar, U.; Muralidharan, N.; Essehli, R.; Amin, R.; Belharouak, I. *Energy Storage Mater.* **2021,** *38*, 309. doi: 10.1016/j.ensm.2021.03.015

(17) Woo, S. U.; Yoon, C. S.; Amine, K.; Belharouak, I.; Sun, Y. K. *J. Electrochem. Soc.* **2007,** *154*, A1005. doi: 10.1149/1.2776160

(18) Ahmed, B.; Xia, C.; Alshareef, H. N. *Nano Today* **2016,** *11*, 250. doi: 10.1016/j.nantod.2016.04.004

(19) Li, W.; Liu, X.; Celio, H.; Smith, P.; Dolocan, A.; Chi, M.; Manthiram, A. *Adv. Energy Mater.* **2018,** *8*, 1703154. doi: 10.1002/aenm.201703154

(20) You, Y.; Celio, H.; Li, J.; Dolocan, A.; Manthiram, A. *Angew. Chem. Int. Ed.* **2018,** *57*, 6480. doi: 10.1002/anie.201801533

(21) Gao, S.; Zhan, X.; Cheng, Y.-T. *J. Power Sources* **2019,** *410–411*, 45. doi: 10.1016/j.jpowsour.2018.10.094

(22) Shu, Y.; Xie, Y.; Yan, W.; Meng, S.; Sun, D.; Jin, Y.; Xiang, L. *Ceramics Int.* **2020,** *46*, 14840. doi: 10.1016/j.ceramint.2020.03.009

(23) Mou, J.; Deng, Y.; He, L.; Zheng, Q.; Jiang, N.; Lin, D. *Electrochim. Acta* **2018,** *260*, 101. doi: 10.1016/j.electacta.2017.11.059

(24) Cao, G.; Jin, Z.; Zhu, J.; Li, Y.; Xu, B.; Xiong, Y.; Yang, J. *J. Alloys Compd.* **2020,** *832*, 153788. doi: 10.1016/j.jallcom.2020.153788

(25) Zhang, Z.; Yang, J.; Huang, W.; Wang, H.; Zhou, W.; Li, Y.; Li, Y.; Xu, J.; Huang, W.; Chiu, W.; *et al. Matter* **2021,** *4*, 302. doi: 10.1016/j.matt.2020.10.021

(26) Chen, D.; Mahmoud, M. A.; Wang, J.-H.; Waller, G. H.; Zhao, B.; Qu, C.; El-Sayed, M. A.; Liu, M. *Nano Lett.* **2019,** *19*, 2037. doi: 10.1021/acs.nanolett.9b00179

(27) Wang, S.; Dai, A.; Cao, Y.; Yang, H.; Khalil, A.; Lu, J.; Li, H.; Ai, X. *J. Mater. Chem. A* **2021,** *9*, 11623. doi: 10.1039/D1TA02563E

(28) Thomas, M. G. S. R.; Bruce, P. G.; Goodenough, J. B. *J. Electrochem. Soc.* **1985,** *132*, 1521. doi: 10.1149/1.2114158

(29) Kanamura, K.; Toriyama, S.; Shiraishi, S.; Ohashi, M.; Takehara, Z.-I. *J. Electroanal. Chem.* **1996,** *419*, 77. doi: 10.1016/S0022-0728(96)04862-0

(30) Zhou, Q.; Ma, J.; Dong, S.; Li, X.; Cui, G. *Adv. Mater.* **2019,** *31*, 1902029. doi: 10.1002/adma.201902029

(31) Aikens, D. A. *J. Chem. Edu.* **1983,** *60*, A25. doi: 10.1021/ed060pA25.1

(32) Fang, S.; Jackson, D.; Dreibelbis, M. L.; Kuech, T. F.; Hamers, R. J. *J. Power Sources* **2018,** *373*, 184. doi: 10.1016/j.jpowsour.2017.09.050

(33) Zhang, J.-N.; Li, Q.; Wang, Y.; Zheng, J.; Yu, X.; Li, H. *Energy Storage Mater.* **2018,** *14*, 1. doi: 10.1016/j.ensm.2018.02.016

(34) Zhang, Z.; Qin, C.; Wang, K.; Han, X.; Li, J.; Sui, M.; Yan, P. *J. Energy Chem.* **2023,** *81*, 192. doi: 10.1016/j.jechem.2023.01.046

(35) Zhou, Y.-N.; Ma, J.; Hu, E.; Yu, X.; Gu, L.; Nam, K.-W.; Chen, L.; Wang, Z.; Yang, X.-Q. *Nat. Commun.* **2014,** *5*, 5381. doi: 10.1038/ncomms6381

(36) Chen, M.; Wang, W.; Shi, Z.; Liu, Z.; Shen, C. *Appl. Surf. Sci.* **2022,** *600*, 154119. doi: 10.1016/j.apsusc.2022.154119

(37) Tallman, K. R.; Wheeler, G. P.; Kern, C. J.; Stavitski, E.; Tong, X.; Takeuchi, K. J.; Marschilok, A. C.; Bock, D. C.; Takeuchi, E. S. *J. Phys. Chem. C* **2021,** *125*, 58. doi: 10.1021/acs.jpcc.0c08095

(38) Yang, Y.; Wang, H.; Zhu, C.; Ma, J. *Angew. Chem. Int. Ed.* **2023,** *62*, e202300057. doi: 10.1002/anie.202300057

(39) Liu, J.; Wu, M.; Li, X.; Wu, D.; Wang, H.; Huang, J.; Ma, J. *Adv. Energy Mater.* **2023,** *13*, 2300084. doi: 10.1002/aenm.202300084

(40) Frisch, M. J.; Trucks, G. W.; Schlegel, H. B.; Scuseria, G. E.; Robb, M. A.; Cheeseman, J. R.; Scalmani, G.; Barone, V.; Petersson, G. A.; Nakatsuji, H.; *et al. Gaussian 16 Rev. B.01*, Wallingford, CT, 2016.

(41) Neese, F. *WIREs Comput. Mol. Sci.* **2018,** *8*, e1327. doi: 10.1002/wcms.1327

(42) Perdew, J. P.; Burke, K.; Ernzerhof, M. *Phys. Rev. Lett.* **1996,** *77*, 3865. doi: 10.1103/PhysRevLett.77.3865

(43) Hutter, J.; Iannuzzi, M.; Schiffmann, F.; VandeVondele, J. *WIREs Comput. Mol. Sci.* **2014,** *4*, 15. doi: 10.1002/wcms.1159

(44) Fan, X.; Chen, L.; Borodin, O.; Ji, X.; Chen, J.; Hou, S.; Deng, T.; Zheng, J.; Yang, C.; Liou, S.-C.; *et al. Nat. Nanotechnol.* **2018,** *13*, 715. doi: 10.1038/s41565-018-0183-2

(45) Li, X.; Liu, J.; He, J.; Wang, H.; Qi, S.; Wu, D.; Huang, J.; Li, F.; Hu, W.; Ma, J. *Adv. Funct. Mater.* **2021,** *31*, 2104395. doi: 10.1002/adfm.202104395

(46) Kim, S. C.; Oyakhire, S. T.; Athanitis, C.; Wang, J.; Zhang, Z.; Zhang, W.; Boyle, D. T.; Kim, M. S.; Yu, Z.; Gao, X.; *et al. Proc. Natl. Acad. Sci.* **2023,** *120*, e2214357120. doi: 10.1073/pnas.2214357120

(47) Zhao, L.; Chen, G.; Weng, Y.; Yan, T.; Shi, L.; An, Z.; Zhang, D. *Chem. Eng. J.* **2020,** *401*, 126138. doi: 10.1016/j.cej.2020.126138

(48) Qiao, Y.; Zhou, Z.; Chen, Z.; Du, S.; Cheng, Q.; Zhai, H.; Fritz, N. J.; Du, Q.; Yang, Y. *Nano Energy* **2018,** *45*, 68. doi: 10.1016/j.nanoen.2017.12.036

(49) Wu, Z.; Li, R.; Zhang, S.; lv, L.; Deng, T.; Zhang, H.; Zhang, R.; Liu, J.; Ding, S.; Fan, L.; *et al. Chem* **2023,** *9*, 650. doi: 10.1016/j.chempr.2022.10.027

(50) Li, X.; Zhang, K.; Mitlin, D.; Paek, E.; Wang, M.; Jiang, F.; Huang, Y.; Yang, Z.; Gong, Y.; Gu, L.; *et al. Small* **2018,** *14*, 1802570. doi: 10.1002/smll.201802570

(51) Bai, Y.; Jiang, K.; Sun, S.; Wu, Q.; Lu, X.; Wan, N. *Electrochim. Acta* **2014,** *134*, 347. doi: 10.1016/j.electacta.2014.04.155

(52) Yao, L.; Liang, F.; Jin, J.; Chowdari, B. V. R.; Yang, J.; Wen, Z. *Chem. Eng. J.* **2020,** *389*, 124403. doi: 10.1016/j.cej.2020.124403

(53) Gao, X.-W.; Deng, Y.-F.; Wexler, D.; Chen, G.-H.; Chou, S.-L.; Liu, H.-K.; Shi, Z.-C.; Wang, J.-Z. *J. Mater. Chem. A* **2015,** *3*, 404. doi: 10.1039/C4TA04018J

(54) Ding, J.-F.; Xu, R.; Yao, N.; Chen, X.; Xiao, Y.; Yao, Y.-X.; Yan, C.; Xie, J.; Huang, J.-Q. *Angew. Chem. Int. Ed.* **2021,** *60*, 11442. doi: 10.1002/anie.202101627

(55) Wang, Z.; Zhu, C.; Liu, J.; Hu, X.; Yang, Y.; Qi, S.; Wang, H.; Wu, D.; Huang, J.; He, P.; *et al. Adv. Funct. Mater.* **2023,** *33*, 2212150. doi: 10.1002/adfm.202212150

(56) Huang, J.; Liu, J.; He, J.; Wu, M.; Qi, S.; Wang, H.; Li, F.; Ma, J. *Angew. Chem. Int. Ed.* **2021,** *60*, 20717. doi: 10.1002/anie.202107957

(57) Jiang, G.; Liu, J.; Wang, Z.; Ma, J. *Adv. Funct. Mater.* **2023,** 2300629. doi: 10.1002/adfm.202300629

(58) Rath, P. C.; Wang, Y.-W.; Patra, J.; Umesh, B.; Yeh, T.-J.; Okada, S.; Li, J.; Chang, J.-K. *Chem. Eng. J.* **2021,** *415*, 128904. doi: 10.1016/j.cej.2021.128904

(59) Zheng, X.; Liao, Y.; Zhang, Z.; Zhu, J.; Ren, F.; He, H.; Xiang, Y.; Zheng, Y.; Yang, Y. *J. Energy Chem.* **2020,** *42*, 62. doi: 10.1016/j.jechem.2019.05.023

(60) Etacheri, V.; Haik, O.; Goffer, Y.; Roberts, G. A.; Stefan, I. C.; Fasching, R.; Aurbach, D. *Langmuir* **2012,** *28*, 965. doi: 10.1021/la203712s

(61) Xia, J.; Petibon, R.; Xiao, A.; Lamanna, W. M.; Dahn, J. R. *J. Electrochem. Soc.* **2016,** *163*, A1637. doi: 10.1149/2.0831608jes

(62) Fan, X.; Wang, C. *Chem. Soc. Rev.* **2021,** *50*, 10486. doi: 10.1039/D1CS00450F

(63) Xu, N.; Shi, J.; Liu, G.; Yang, X.; Zheng, J.; Zhang, Z.; Yang, Y. *J. Power Sources Adv.* **2021,** *7*, 100043. doi: 10.1016/j.powera.2020.100043

(64) Wang, T.; Rao, L.; Jiao, X.; Choi, J.; Yap, J.; Kim, J.-H. *ACS Appl. Energy Mater.* **2022,** *5*, 7346. doi: 10.1021/acsaem.2c00861

(65) Song, Y.; Mao, Q.; Li, Q.; Huang, Z.; Wan, Y.; Hong, B.; Zhong, Q. *ACS Appl. Energy Mater.* **2023,** *6*, 4271. doi: 10.1021/acsaem.3c00196

(66) Wu, F.; Schür, A. R.; Kim, G.-T.; Dong, X.; Kuenzel, M.; Diemant, T.; D'Orsi, G.; Simonetti, E.; De Francesco, M.; Bellusci, M.; *et al. Energy Storage Mater.* **2021,** *42*, 826. doi: 10.1016/j.ensm.2021.08.030

(67) Xu, M.; Liu, Y.; Li, B.; Li, W.; Li, X.; Hu, S. *Electrochem. Commun.* **2012,** *18*, 123. doi: 10.1016/j.elecom.2012.02.037

(68) Pham, T. D.; Faheem, A. B.; Kim, J.; Kwak, K.; Lee, K.-K. *Electrochim. Acta* **2023**, 142496. doi: 10.1016/j.electacta.2023.142496

(69) Winter, E.; Briccola, M.; Schmidt, T. J.; Trabesinger, S. *Appl. Res.* **2022,** e202200096. doi: 10.1002/appl.202200096

(70) Ma, Q.; Zhang, X.; Wang, A.; Xia, Y.; Liu, X.; Luo, J. *Adv. Funct. Mater.* **2020,** *30*, 2002824. doi: 10.1002/adfm.202002824

(71) Yang, Y.-P.; Jiang, J.-C.; Huang, A.-C.; Tang, Y.; Liu, Y.-C.; Xie, L.-J.; Zhang, C.-Z.; Wu, Z.-H.; Xing, Z.-X.; Yu, F. *Process Saf. Environ. Prot.* **2022,** *160*, 80. doi: 10.1016/j.psep.2022.02.018

(72) Zhang, C.-M.; Li, F.; Zhu, X.-Q.; Yu, J.-G. *Molecules* **2022**, 27, 3107; doi: 10.3390/molecules27103107

(73) Li, Y.; Li, W.; Shimizu, R.; Cheng, D.; Nguyen, H.; Paulsen, J.; Kumakura, S.; Zhang, M.; Meng, Y. S. *Adv. Energy Mater.* **2022,** *12*, 2103033. doi: 10.1002/aenm.202103033

(74) Martinez, A. C.; Rigaud, S.; Grugeon, S.; Tran-Van, P.; Armand, M.; Cailleu, D.; Pilard, S.; Laruelle, S. *Electrochim. Acta* **2022,** *426*, 140765. doi: 10.1016/j.electacta.2022.140765

(75) Fu, A.; Lin, J.; Zhang, Z.; Xu, C.; Zou, Y.; Liu, C.; Yan, P.; Wu, D.-Y.; Yang, Y.; Zheng, J. *ACS Energy Lett.* **2022,** *7*, 1364. doi: 10.1021/acsenergylett.2c00316

(76) Xu, M.; Zhou, L.; Dong, Y.; Chen, Y.; Garsuch, A.; Lucht, B. L. *J. Electrochem. Soc.* **2013,** *160*, A2005. doi: 10.1149/2.053311jes

(77) Xu, M.; Zhou, L.; Dong, Y.; Chen, Y.; Demeaux, J.; MacIntosh, A. D.; Garsuch, A.; Lucht, B. L. *Energy Environ. Sci.* **2016,** *9*, 1308. doi: 10.1039/C5EE03360H

(78) Yang, X.; Lin, M.; Zheng, G.; Wu, J.; Wang, X.; Ren, F.; Zhang, W.; Liao, Y.; Zhao, W.; Zhang, Z.; *et al. Adv. Funct. Mater.* **2020,** *30*, 2004664. doi: 10.1002/adfm.202004664

(79) Liu, F.; Zhang, Z.; Yu, Z.; Fan, X.; Yi, M.; Bai, M.; Song, Y.; Mao, Q.; Hong, B.; Zhang, Z.; *et al. Chem. Eng. J.* **2022,** *434*, 134745. doi: 10.1016/j.cej.2022.134745

(80) Zhang, Q.-K.; Zhang, X.-Q.; Wan, J.; Yao, N.; Song, T.-L.; Xie, J.; Hou, L.-P.; Zhou, M.-Y.; Chen, X.; Li, B.-Q.; *et al. Nat. Energy* **2023,** *8*, 725. doi: 10.1038/s41560-023-01275-y